

# Synthesis of Alternate Copolymers Composed of Dithienosilole and $\pi$ -Conjugated Units

By Joji OHSHTA,\* Hiroyuki KAI, Keisuke KIMURA, Kwang-Hoi LEE, and Atsutaka KUNAI

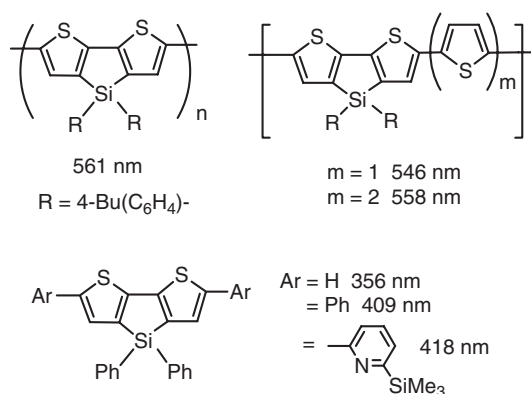
Stille cross-coupling reactions of 2,6-bis(tributylstannyl)-4,4-bis(4-butylphenyl)dithienosilole with dihaloarenes gave dithienosilole-arene alternate polymers. The resulting copolymers showed the UV absorption and emission maxima at 450–601 nm and 543–698 nm, respectively, depending on the arene units in the polymer backbone. Electroluminescence properties of the dithienosilole-pyridine polymer were studied in its spin-coated film.

KEY WORDS: Silole / Electroluminescence / Conjugated Polymer / Thiophene /

Recently, we demonstrated that dithienosilole having a silole ring condensed with a bithiophene system (DTS in Scheme 1) exhibits enhanced conjugation, as compared with silole-free bithiophene.<sup>1–3</sup> The tricyclic system makes the thiophene rings retain high coplanarity, enhancing the  $\pi$ -conjugation in DTS. In addition, bonding interaction between the silicon  $\sigma^*$ -orbital and the bithiophene  $\pi^*$ -orbital ( $\sigma^*$ - $\pi^*$  conjugation)<sup>2</sup> lowers the LUMO energy, which allows the use of the DTS-based compounds as efficient electron transporting materials for multi-layered organic light emitting diodes (OLEDs).<sup>3</sup> It was also found that DTS-based compounds bearing appropriate substituents, such as methylthio groups, are usable as hole-transport materials in OLEDs.<sup>4</sup>

Recently, palladium-catalyzed oxidative coupling of 2,6-bis(tributylstannyl)dithienosilole proved to produce poly(dithienosilole-2,6-diyl)s cleanly.<sup>5,6</sup> These DTS homopolymers exhibit efficient conjugation in the polymer backbone. For example, UV absorption maximum of poly[4,4-bis(4-butylphenyl)dithienosilole-2,6-diyl] appears at 561 nm, red-shifted from that of regio-regular poly(3-hexylthiophene) (HT > 95%), by about 100 nm. It was also demonstrated that DTS-thiophene and bithiophene copolymers could be used as hole-transport emitters for OLEDs<sup>5</sup> and p-type semiconductors.<sup>7</sup> DTS-fluorene<sup>8,9</sup> and DTS-dithienylenebenzothiadiazole<sup>6</sup> copolymers were also synthesized recently, as photoluminescence and photovoltaic-active materials, respectively.

To know how the electronic states of DTS-containing  $\pi$ -conjugated polymers are affected by the structure, we prepared alternate copolymers [DTS-Ar]<sub>n</sub>, by stille coupling reactions of bis(tributylstannyl)-substituted DTS and various dihaloarenes (ArX<sub>2</sub>), dibromo-benzene, biphenyl, pyridine, and tetraphenylsilole, and diiodoquinoxaline. The present polymer with Ar = pyridine unit showed electroluminescence properties, although the efficiency was rather low.



Scheme 1. UV absorption maxima of DTS-containing compounds (refs 2, 3, and 5).

## EXPERIMENTAL

### General Procedure

All reactions were carried out in dry nitrogen. Toluene was distilled from Na and stored over activated molecular sieves at ambient temperature until use. Monomer **DTS-Sn** was prepared as reported in the literature.<sup>5</sup> GPC analysis of the polymers was performed with Shodex columns, KF804 and KF806 connected in series, using a UV detector (240 nm). NMR spectra were measured on a JEOL model LA-400 spectrometer. Some <sup>13</sup>C NMR signals of the polymers are missing, because of the signal broadness and rather low solubility of the polymers.

### Preparation of DTS-containing Polymers

In a 30 mL two necked flask was placed **DTS-Sn** and a dihaloarene (0.1 mmol each), 4 mg (5 mol %) of Pd(PPh<sub>3</sub>)<sub>4</sub>, 1 mg (5 mol %) of CuI, and 2 mL of toluene. After the mixture was heated for 24 h at the reflux temperature, 10 mL of chloroform was added and the resulting mixture was filtered.

Department of Applied Chemistry, Graduate School of Engineering, Hiroshima University, Higashi-Hiroshima 739-8527, Japan

\*To whom correspondence should be addressed (Tel: +81-82-424-7743, Fax: +81-82-424-5494, E-mail: jo@hiroshima-u.ac.jp).

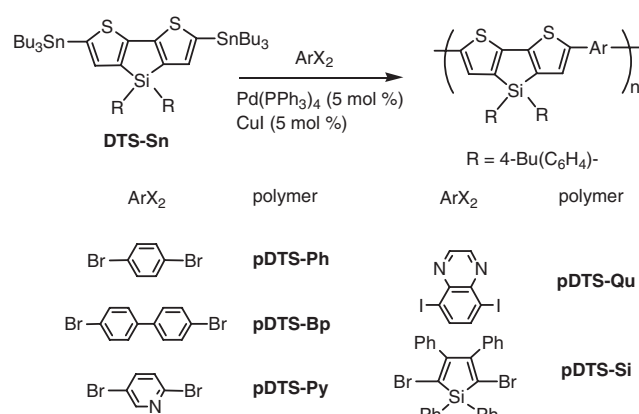
The solvent was evaporated and the residue was reprecipitated from chloroform-hexane to give the corresponding polymer as a powder. Data for **pDTS-Ph**: dark red solid; mp >300 °C; <sup>1</sup>H NMR ( $\delta$  in CDCl<sub>3</sub>) 0.90 (br t, 6H,  $J$  = 7.34 Hz, CH<sub>2</sub>CH<sub>2</sub>CH<sub>2</sub>CH<sub>3</sub>), 1.31–1.37 (br m, 4H, CH<sub>2</sub>CH<sub>2</sub>CH<sub>2</sub>CH<sub>3</sub>), 1.56–1.60 (br m, 4H, CH<sub>2</sub>CH<sub>2</sub>CH<sub>2</sub>CH<sub>3</sub>), 2.60 (br t,  $J$  = 7.08 Hz, CH<sub>2</sub>CH<sub>2</sub>CH<sub>2</sub>CH<sub>3</sub>), 7.18 (br d, 2H,  $J$  = 6.2 Hz, phenylene protons), 7.22 (br d, 2H,  $J$  = 6.2 Hz, phenylene protons), 7.32–7.67 (m, 10H, DTS and phenylene protons); <sup>13</sup>C NMR ( $\delta$  in CDCl<sub>3</sub>) 13.91, 22.36, 33.43, 35.76, 125.86, 128.46, 128.90, 132.00, 132.15, 133.26, 135.47, 141.60, 145.50, 149.33. Data for **p-DTS-Bp**: red solid; mp >300 °C; <sup>1</sup>H NMR ( $\delta$  in CDCl<sub>3</sub>) 0.90 (br t, 6H,  $J$  = 7.02 Hz, CH<sub>2</sub>CH<sub>2</sub>CH<sub>2</sub>CH<sub>3</sub>), 1.29–1.35 (br m, 4H, CH<sub>2</sub>CH<sub>2</sub>CH<sub>2</sub>CH<sub>3</sub>), 1.53–1.57 (br m, 4H, CH<sub>2</sub>CH<sub>2</sub>CH<sub>2</sub>CH<sub>3</sub>), 2.61 (br t,  $J$  = 7.93 Hz, CH<sub>2</sub>CH<sub>2</sub>CH<sub>2</sub>CH<sub>3</sub>), 7.21 (br s, 4H, phenylene protons), 7.23–7.61 (m, 14H, phenylene and DTS protons); <sup>13</sup>C NMR ( $\delta$  in CDCl<sub>3</sub>) 13.93, 22.36, 33.43, 35.76, 125.95, 127.17, 128.14, 128.46, 128.91, 129.29, 133.55, 135.49, 137.88, 141.69, 145.50, 149.45. Data for **pDTS-Py**: dark red solid; mp >300 °C; <sup>1</sup>H NMR ( $\delta$  in CDCl<sub>3</sub>) 0.91 (br s, 6H, CH<sub>2</sub>CH<sub>2</sub>CH<sub>2</sub>CH<sub>3</sub>), 1.34 (br s, 4H, CH<sub>2</sub>CH<sub>2</sub>CH<sub>2</sub>CH<sub>3</sub>), 1.58 (br s, 4H, CH<sub>2</sub>CH<sub>2</sub>CH<sub>2</sub>CH<sub>3</sub>), 2.62 (br s, 4H, CH<sub>2</sub>CH<sub>2</sub>CH<sub>2</sub>CH<sub>3</sub>), 7.23–7.88 (m, 10H, DTS, phenylene and pyridylene protons), 8.55 (br s, 0.6H, Br-pyridyl), 8.75 (br s, 0.3H, pyridylene proton on C6); <sup>13</sup>C NMR ( $\delta$  in CDCl<sub>3</sub>) 13.90, 22.32, 33.41, 35.74, 117.8, 119.6, 128.50, 130.82, 131.92, 134.45, 135.43, 138.9, 145.62, 150.44, 151.01. Data for **pDTS-Qu**: blue purple solid; mp >300 °C; <sup>1</sup>H NMR ( $\delta$  in CDCl<sub>3</sub>) 0.88–0.93 (br m, 6H, CH<sub>2</sub>CH<sub>2</sub>CH<sub>2</sub>CH<sub>3</sub>), 1.25–1.36 (br m, 4H, CH<sub>2</sub>CH<sub>2</sub>CH<sub>2</sub>CH<sub>3</sub>), 1.64 (br s, 4H, CH<sub>2</sub>CH<sub>2</sub>CH<sub>2</sub>CH<sub>3</sub>), 2.61 (br s, 4H, CH<sub>2</sub>CH<sub>2</sub>CH<sub>2</sub>CH<sub>3</sub>), 7.15–7.95 (m, 10H, DTS and phenylene protons), 7.95–8.21 (m, 2H, quinoxaline protons on C2 and C3), 8.95 (br s, 2H, quinoxaline protons on C6 and C7); <sup>13</sup>C NMR ( $\delta$  in CDCl<sub>3</sub>) 13.93, 22.37, 33.46, 35.77, 126.64, 128.89, 135.58, 139.53, 139.72, 140.23, 142.95, 145.15, 145.41. Data for **p-DTS-Si**: blue purple solid; mp 254–257 °C; <sup>1</sup>H NMR ( $\delta$  in CDCl<sub>3</sub>) 0.93 (br s, 6H, CH<sub>2</sub>CH<sub>2</sub>CH<sub>2</sub>CH<sub>3</sub>), 1.35 (br s, 4H, CH<sub>2</sub>CH<sub>2</sub>CH<sub>2</sub>CH<sub>3</sub>), 1.55 (br s, 4H, CH<sub>2</sub>CH<sub>2</sub>CH<sub>2</sub>CH<sub>3</sub>), 2.58 (br s, 4H, CH<sub>2</sub>CH<sub>2</sub>CH<sub>2</sub>CH<sub>3</sub>), 7.01–7.79 (m, 37H, DTS, phenylene and phenyl protons); <sup>13</sup>C NMR ( $\delta$  in CDCl<sub>3</sub>) 13.93, 22.32, 33.43, 35.71 (Bu), 125.45, 127.28, 127.51, 128.21, 128.79, 129.63, 131.81, 135.09, 136.24, 138.85, 144.74.

### Fabrication of OLED

A thin film of **pDTS-Py** was prepared by spin-coating from a solution of polymer in chloroform (2 g/L) on an anode, ITO coated on a glass substrate at 2000 rpm. A layer of magnesium-silver alloy with an atomic ratio of 10:1 (200 nm) and silver (100 nm) were deposited on the polymer layer surface, in this order, as the cathode at  $1 \times 10^{-5}$  torr.

## RESULTS AND DISCUSSION

Polymers composed of DTS-Ar alternate units were pre-



Scheme 2.

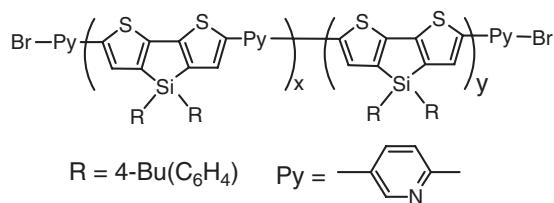
Table I. Synthesis and Properties of Polymers

polymer	yield (%) <sup>a</sup>	$M_n^{a,b}$	$M_w/M_n^{a,b}$	abs $\lambda_{\text{max}}$ (nm)		em $\lambda_{\text{max}}$ (nm)	
				in THF	film	in THF	film
<b>pDTS-Ph</b>	47	4000	1.3	482	488	573	626
<b>pDTS-Bp</b>	29	4300	1.3	450	460	543	602
<b>pDTS-Py</b>	38	3100	1.3	460	473	564	631
<b>pDTS-Qu</b>	57	4500	1.4	583	630	698	721
<b>p-DTS-Si</b>	32	4200	1.1	601	607	— <sup>c</sup>	— <sup>c</sup>

<sup>a</sup>After reprecipitation from ethanol. <sup>b</sup>Determined by GPC, relative to polystyrene standards. <sup>c</sup>No emission detected.

pared by the Stille coupling reactions of 2,6-bis(tributylstannyl)-4,4-bis(4-butylphenyl)dithienosilole (**DTS-Sn**) and dihaloarenes ( $\text{ArX}_2$ ) in moderate yields, as shown in Scheme 2 and Table I. For the preparation of quinoxaline-containing polymer **pDTS-Qu**, diiodoquinoxaline must be used as the monomer. No polymerization occurred, when dibromoquinoxaline was employed as the monomer instead of the diiodo derivative, due to the low activity of the dibromide. The polymer structures were verified by their <sup>1</sup>H and <sup>13</sup>C NMR spectra. Although these spectra show rather broad signals accompanied with some unidentified signals with low intensities, the integration ratios of the <sup>1</sup>H NMR signals are almost consistent with those expected for the regularly alternate structures shown in Scheme 2, except for **pDTS-Py**. For **pDTS-Py**, two signals due to pyridine ring protons on C2 are observed in the NMR spectrum at 8.55 and 8.78 ppm, which are assignable to those of pyridylene units in the polymer chain and the terminal bromopyridyl units, respectively, by comparison with the literature data.<sup>10</sup> The NMR integration ratio of the pyridylene ring proton at 8.55 ppm versus butyl protons was found to be only about 0.3/18, indicating that homo coupling reactions were involved to an extent in this polymerization, giving a DTS-rich structure shown in Scheme 3 with  $x/y = ca. 22/78$ .

These polymers were obtained as red to blue-purple solids. They are soluble in common organic solvents, such as chloroform and THF, but insoluble in hexane and ethanol, and can be spin-coated to thin solid films. Optical properties of these copolymers are also summarized in Table I. As can be



**Scheme 3.** Structure of pDTS-Py.

seen in Table I, UV absorption and emission bands of the present polymers are at lower energies in films than in solutions, as often observed for highly conjugated polymers. This is due to the higher co-planarity of the conjugated units in the polymer backbone and/or interchain  $\pi$ - $\pi$  interaction in the solid states. These polymers show red-shifted absorption and emission maxima, relative to monomeric DTS compounds (see Scheme 1).<sup>1-3</sup> However, both the absorption and emission maxima of **pDTS-Ph**, **pDTS-Bp**, and **pDTS-Py** appear at shorter wavelength than those of **p-DTS**, indicating that introduction of phenylene and pyridylene units into the backbone rather interrupts the conjugation, like DTS-thienylene alternate polymers, reported previously (Scheme 1).<sup>5</sup> In contrast, polymers **pDTS-Qu** and **pDTS-Si** exhibited the absorption maxima at much longer wavelengths than **p-DTS**. This is probably due to donor-acceptor (D-A) type interaction between DTS (D) and quinoxaline/silole (A) units. In fact, solvatochromic behavior with respect to the emission spectra was observed for **pDTS-Qu**, and the band at 698 nm in THF moved to 680 nm in toluene. Since no significant changes were found in the UV absorption spectra depending on the solvent ( $\lambda_{\text{max}} = 583$  nm in THF and 580 nm in toluene), the large solvatochromic emission spectral shift seems to reflect the polar character of **pDTS-Qu** at the excited state. In contrast, **pDTS-Ph** and **pDTS-Bp** showed only 1–2 nm blue shifts of the emission bands, when the solvent was changed from THF to toluene. To know more about the D-A type interaction, we carried out DFT calculations on a model compound (**DTS-Qu**) and the HOMO and LUMO profiles derived from the calculations are depicted in Figure 1.<sup>11</sup> The HOMO of **DTS-Qu** is rather localized on the DTS unit, while its LUMO primarily lies on the Qu unit, indicating the polarized structure in the excited state.

We next examined the present polymers as OLED materials. Of those, **pDTS-Py** exhibited electroluminescence (EL) properties in its spin-coated film and red emission was observed from the single-layered device with the structure of ITO (indium tin oxide)/**pDTS-Py**/Mg-Ag. The EL spectrum showed a broad band centered about 650 nm, a little red shifted from the emission band of the polymer film ( $\lambda_{\text{em}} = 631$  nm), as can be seen in Figure 2. The maximum luminance from the device was approximately 7 cd/m<sup>2</sup>. Other DTS-Ar polymers did not show EL properties in their single-layered devices. Previously, we reported that a DTS-thienylene polymer was electroluminescent in the single-layered device with the maximum luminance of 6 cd/m<sup>2</sup>, while DTS homo

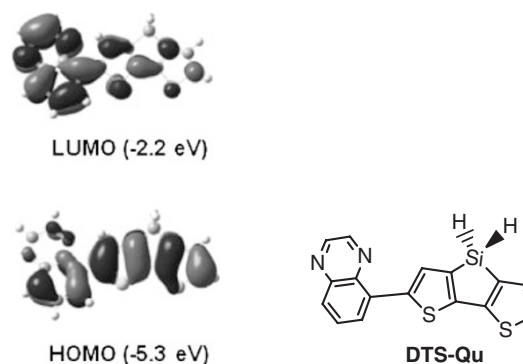


**Figure 1.** HOMO and LUMO profiles of DTS-Qu derived from DFT calculations at the level of B3LYP/6-31G(d).

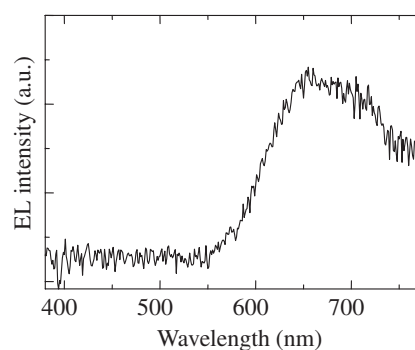


**Figure 2.** EL spectrum from the device of ITO/pDTS-Py/Mg-Ag.

polymer was not (Scheme 1).<sup>5</sup> Presumably, two substituents on the DTS silicon atom cover the  $\pi$ -conjugated system, which suppress carrier hopping between the polymer chains through  $\pi$ - $\pi$  stacking. Introducing a flat  $\pi$ -conjugated unit (Ar) with an appropriate size and a ratio (DTS/Ar) would be important to enhance the interchain hopping, although we have not obtained clear explanation for the relationship between the polymer structures and their electroluminescence properties.

In conclusion, we prepared alternate polymers composed of DTS and aromatic units. It was demonstrated that the UV absorption and emission maxima of the present DTS-Ar copolymers range widely from 450 to 600 nm for absorption and from 540 to 700 nm for emission, respectively, depending on the nature of the Ar group in the polymer backbone. In particular, introduction of electron-withdrawing Ar units led to large red-shifts, probably due to the D-A type interaction in the polymer backbone. We found also that the pyridine-containing polymer showed EL properties. However, the efficiency was still low and further investigation to optimize the device structure seems to be necessary.

**Acknowledgment.** This work was supported by the Grant-in-Aid for Scientific Research on the Priority Area “Super-Hierarchical Structures” by the Ministry of Education, Culture, Sports, Science, and Technology of Japan, to which our thanks are due.

Received: October 29, 2008  
Accepted: February 22, 2009  
Published: April 8, 2009

## REFERENCES

1. J. Ohshita, M. Nodono, T. Watanabe, Y. Ueno, A. Kunai, Y. Harima, K. Yamashita, and M. Ishikawa, *J. Organomet. Chem.*, **553**, 487 (1998).
2. J. Ohshita, M. Nodono, H. Kai, T. Watanabe, A. Kunai, K. Komaguchi, M. Shiotani, A. Adachi, K. Okita, Y. Harima, K. Yamashita, and M. Ishikawa, *Organometallics*, **18**, 1453 (1999).
3. J. Ohshita, H. Kai, A. Takata, T. Iida, A. Kunai, N. Ohta, K. Komaguchi, M. Shiotani, A. Adachi, K. Sakamaki, and K. Okita, *Organometallics*, **20**, 4800 (2001).
4. K.-H. Lee, J. Ohshita, and A. Kunai, *Organometallics*, **23**, 5481 (2004).
5. J. Ohshita, K. Kimura, K.-H. Lee, A. Kunai, Y.-W. Kwak, E.-C. Son, and Y. Kunugi, *J. Polym. Sci., Part A: Polym. Chem.*, **45**, 4588 (2007).
6. L. Liao, L. Dai, A. Smith, M. Durstock, J. Lu, J. Ding, and Y. Tao, *Macromolecules*, **40**, 9406 (2007).
7. H. Usta, G. Lu, A. Facchetti, and T. J. Marks, *J. Am. Chem. Soc.*, **128**, 9034 (2006).
8. M. S. Liu, J. D. Luo, and A. K. Y. Jen, *Chem. Mater.*, **15**, 3496 (2003).
9. Z.-W. Zhang, J. Li, B. Huang, and J. G. Qin, *Chem. Lett.*, **35**, 958 (2006).
10. I. J. Jenkins, U. Salzner, and P. G. Pickup, *Chem. Mater.*, **8**, 2444 (1996).
11. Gaussian 03: M. J. Frisch, G. W. Trucks, H. B. Schlegel, G. E. Scuseria, M. A. Robb, J. R. Cheeseman, V. G. Zakrzewski, J. A., Jr. Montgomery, R. E. Stratmann, J. C. Burant, S. Dapprich, J. M. Millam, A. D. Daniels, K. N. Kudin, M. C. Strain, O. Farkas, J. Tomasi, V. Barone, M. Cossi, R. Cammi, B. Mennucci, C. Pomelli, C. Adamo, S. Clifford, J. Ochterski, G. A. Petersson, P. Y. Ayala, Q. Cui, K. Morokuma, D. K. Maliek, A. D. Rabuck, K. Raghavachari, J. B. Foresman, J. Cioslowski, J. V. Ortiz, B. B. Stefanov, G. Liu, A. Liashenko, P. Piskorz, I. Komaromi, R. Gomperts, R. L. Martin, D. J. Fox, T. Keith, M. A. Al-Lalam, C. Y. Peng, A. Nanayakkara, C. Gonzalez, M. Challacombe, P. M. W. Gill, B. G. Johnson, W. Chen, M. W. Wong, J. L. Andres, M. Head-Gordon, E. S. Replogle, and J. A. Pople, Program Packages from Gaussian Inc., Pittsburgh, PA.